HEAT TRANSFER IN LOW REYNOLDS NUMBER FLOWS THROUGH MINIATURIZED CHANNELS

Oyinlola M.A.* and Shire G.S.F.
*Author for correspondence
Institute of Energy and Sustainable Development,
De Montfort University
Leicester, LE1 9BH
UK
E-mail: muyiwa.oyinlola@dmu.ac.uk

ABSTRACT

The use of miniaturized channels as heat sinks/ heat exchangers is of great importance due to advantages of compact size and high heat sinking capabilities. The small hydraulic diameters of these miniaturized channels imply a higher pressure drop and consequently higher pumping power. Therefore, where possible, the pumping power required may be reduced by running applications at low flow velocities. This paper therefore investigates the heat transfer in low Reynolds number flow through miniaturized channels. Forced convection experiments were performed on 2 instrumented metal plates with 0.5 mm and 0.25 mm deep channels respectively. The channels were 2 mm wide and 270 mm long. A propylene glycol-based heat transfer fluid for solar collectors, Tyfocor® LS, was used as the working fluid. Reynolds numbers were in the range 10 – 100 and fluid inlet temperatures ranged from 5 – 60 °C. The measured Nusselt numbers were observed to depend more on the Peclet number and less on the geometry. Peclet number dependent Nusselt numbers was attributed to miniaturization scaling effects. A correlation for estimating the Nusselt number in terms of the Peclet number and hydraulic diameter was proposed. The results are significant in predicting the heat sinking performance in applications having low Reynolds number flows through miniaturized channels such as compact solar thermal collectors.

INTRODUCTION

Heat transfer and fluid flow in miniaturized (micro or mini) channels has been the focus of many researchers since Tuckerman and Pease [1] pioneered the study of heat transfer in micro-channels over three decades ago. These studies were largely in the context of micro-electronic components. In recent times however, due to advantages of compact size and high heat sinking capabilities, the use of miniaturized channels as heat sinks/ heat exchangers has been extended to other fields such as automotive, chemical and food industries, environmental technology and the aviation and space industries [2]. Kandlikar's [3] definition of conventional channels as those having hydraulic diameters above 3 mm is adopted in this study.

NOMENCLATURE

a	[m]	Channel depth
b	[m]	Channel width
c_p	[J/kg K]	Specific heat capacity
D_h	[m]	Hydraulic diameter
h	[W/m^2 K]	Heat transfer coefficient
k_f	[W/m K]	Thermal conductivity of fluid
L	[m]	Length of channel
L_t	[m]	Thermal entry length
$\dot{m}$	[kg/s]	Mass Flow rate
N_c	[-]	Number of channels in plate
Nu	[-]	Nusselt number
Pe	[-]	Peclet number
Pr	[-]	Prandtl number
Q	[W]	Heat supplied
Re	[-]	Reynolds number
S_c	[m^2]	Total surface area of channels
T_f	[K]	Average fluid temperature
T_{in}	[K]	Fluid temperature at inlet
T_{out}	[K]	Fluid temperature at outlet
T_p	[K]	Average plate temperature
α	[-]	Aspect ratio
ρ	[kg/m^3]	Density
μ	[Pa.s]	Dynamic Viscosity
ν	[m^2/s]	Kinematic viscosity
ΔT_{pf}	[K]	Plate-fluid temperature difference
ω	[-]	Uncertainty

The theory and correlations of heat transfer and fluid flow in conventional sized channels are well established; constant Nusselt number in the range 0.457 – 8.235, with the exact value depending on boundary conditions and geometry, are expected for fully developed laminar flow [4-6]. The results from the extensive studies on heat transfer in miniaturized channels are still inconsistent. Reviews on experimental and numerical studies of heat transfer in miniaturized channels published by [7-9] confirm the very large scatter in published results. These reviews unanimously attribute the dispersion to "scaling effects", which result from neglecting phenomena that are insignificant in conventional sized channels but become significant in flows through miniaturized channel. Examples of these scaling effects include surface roughness[10], entrance and exit effects [11, 12], conjugate heat transfer[13, 14], thermal boundary conditions [15], viscous dissipation[16] and

increased measurement uncertainties [17]. Some of these scaling effects such as entrance effects, conjugate heat transfer, and viscous dissipation are directly affected by the flow velocity, even in the laminar regime [18]. This paper therefore aims to investigate the effects of low Reynolds number flows on the thermal performance.

EXPERIMENTAL APPARATUS

Description of the experimental system

A setup was designed for experimental investigation; Figure 1 shows a flow schematic of the experimental facility; a temperature controlled circulating bath supplied the heat transfer fluid (Tyfocor® LS, a propylene glycol-based heat transfer fluid for solar collectors) at constant flow rate and temperature to a micro-channel test rig. The properties of Tyfocor® LS are presented in Table 1. Instruments to measure the temperature at different points, the pressure drop across the test rig and the mass flow rate were embedded at appropriate locations in the loop.

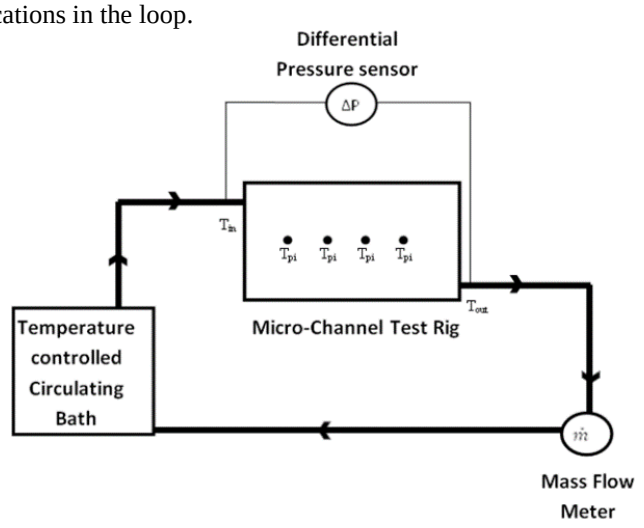

Figure 1 Flow Schematic of experimental facility

The main component of the experimental setup was the micro-channel test rig. It was made up of two 340 × 240 × 10 mm aluminium slabs – a "top" and "bottom" piece, with a thinner (3 mm) channel plate sandwiched between them, as shown in Figure 2. This arrangement allowed a variety of relatively simple channel plates to be tested without each needing its own inlet and outlet connections.

A self-adhesive heater mat, capable of supplying up to 1200 W/m^2, was mounted on the top slab. The results used in this paper were obtained with a heater power of about 70W, equivalent to 950 W/m^2. The temperature profiles obtained showed that the experiment can be approximated as a constant Heat flux boundary condition. The rig was insulated with a box constructed from Polyisocyanurate foam. The channels were arranged in parallel. In order to reduce flow maldistribution the inlet and outlet ports were located at the opposite sides of a diagonal across the channels.

Table 1: Properties of Tyfocor

T °C	ρ kg/m^3	ν mm^2/s	c_p kJ/kg °C	k_f W/m °C	*Pr*
0	1044	15	3.52	0.4	137.81
10	1040	8	3.55	0.406	72.75
20	1033	5	3.6	0.413	45.02
30	1028	3.5	3.64	0.42	31.18
40	1022	2.5	3.68	0.428	21.97
50	1015	1.95	3.72	0.434	16.97
60	1008	1.7	3.76	0.441	14.61
70	1001	1.4	3.8	0.449	11.86
80	994	1.1	3.84	0.455	9.23

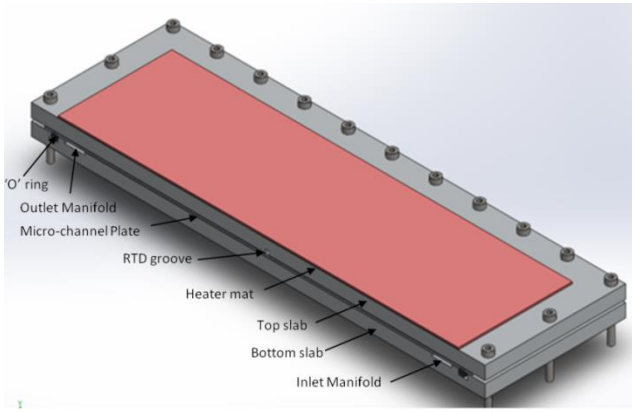

Figure 2: Cross section of test rig

Table 2 shows geometry details of the channels machined on the two plates, Temperatures of the plate at different points (T_{pi}), fluid at inlet (T_{in}) and fluid at outlet (T_{out}) were measured using Type T thermocouples. Several thermocouples were fixed on the absorber plate using fibre-glass thermal attachment pads, as shown in Figure 3. Plate temperature measurements were corrected as outlined in [18]. These corrections were in the range of 0 to –1.5°C, depending on the experimental conditions. Thermocouples were placed inside the inlet and outlet ports after elbow fittings (to promote fluid mixing) for accurate readings of bulk fluid temperature. All pipes and fittings were properly insulated to minimise heat loss to the ambient. The flow rate ($\dot{m}$) and pressure drop (Δp) were measured using a Coriolis mass flow meter and a differential pressure sensor respectively. All the measured quantities were logged with a 16-bit National Instruments data acquisition system via Labview. Thermocouples were connected through a SCXI-1102 thermocouple interface board. Signals were sampled at 2 Hz; signal quality was studied using an oscilloscope to ensure they were clean and free from interference. Post steady state data were used for analyses. The criterion for steady state was defined by $\frac{dT}{dt} < 2.5 \times 10^{-5}$ °C/s; this was reached after approximately 10–

15 minutes at a constant flow rate. The enthalpy change of the fluid was used to calculate the heat flux. The power consumed by the heater mat was measured using a voltmeter and ammeter; the heat flux as defined by flow measurement was within 10% of power consumed.

Table 2 Geometric parameters of the channels

Plate	a (mm)	b (mm)	p (mm)	D_h (mm)	L (mm)	α	N_c
A	0.5	2	3	0.8	270	0.25	60
B	0.25	2	3	0.44	270	0.125	60

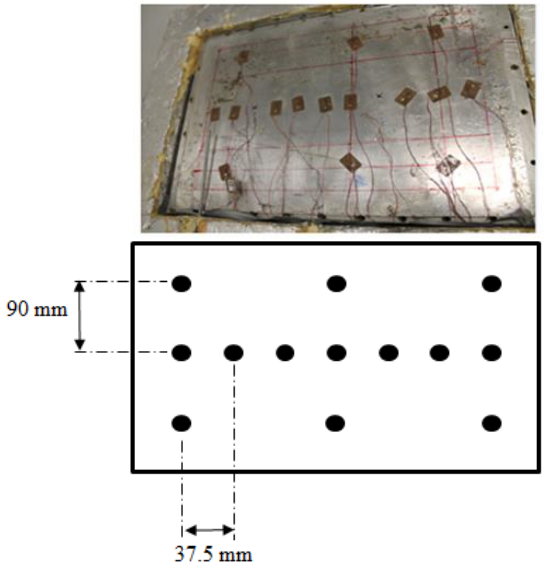

Figure 3 Thermocouple arrangement on plate

Data Reduction and Uncertainty

Each test was run for 15 minutes to reach steady state and 200 data points were then captured. The sample standard deviation was typically 0.016 °C. The parameters presented in Table 3 were calculated using the average of the captured data.

The Data Acquisition system has a function for calibrating all channels. This procedure compensates for the inaccuracies in the whole measurement system. The thermocouples were bonded together, put in the bath and calibrated at a number of temperatures to match bath temperature readout. Voltages from the mass flow meter were calibrated to match its display readout while the differential pressure sensor was calibrated to match a hand held manometer. The mass flow meter was also checked by timing flow into a measuring cylinder.

After calibration, steady state measurements were recorded for about 15 minutes. The standard deviation observed in each parameter was taken as the instrument's uncertainty. Uncertainties in geometric parameters were estimated using high precision measuring instruments as well as manufacturers' specifications. The deviations were used to estimate the uncertainties in the calculated values, assuming that the deviations in each term were uncorrelated. For example, equation (1) [19] was used to estimate the uncertainty in the heat transfer coefficient. Further details can be found in [20].

$$\omega_h = h\left[\left(\frac{\omega_Q}{Q}\right)^2 + \left(\frac{\omega_{S_c}}{S_c}\right)^2 + \left(\frac{\omega_{\Delta T_{pf}}}{\Delta T_{pf}}\right)^2\right]^{1/2} \quad (1)$$

Table 3: Details of data reduction

Parameter	Definition	Equation number	Uncertainty
Aspect ratio	$\alpha = \frac{a}{b}$	(2)	0.05
Reynolds number	$Re = \left(\frac{\dot{m}}{abN_c}\right)\frac{D_h}{\mu}$	(3)	<10%
Mean plate temperature	$T_p = \frac{\sum_{i=1}^{n} T_{pi}}{n}$	(4)	0.06°C
Mean fluid temperature	$T_f = \frac{T_{in} + T_{out}}{2}$	(5)	0.04°C
surface area of channels	$S_c = 2N_c L(a+b)$	(6)	0.00115m^2
Heat transferred to fluid	$Q = \dot{m}C_p\left(T_{out} - T_{in}\right)$	(7)	7W
Heat transfer coefficient	$h = \frac{Q}{S_c\left(T_p - T_f\right)}$	(8)	<20%
Nusselt Number	$Nu = \frac{hD_h}{k_f}$	(9)	<20%
Thermal entry length	$L_t = 0.05 RePrD_h$	(10)	-

RESULTS AND DISCUSSION

Figure 4 shows a plot of Nusselt number against Reynolds number; Firstly, it can be observed that Nusselt numbers show some dependence on Reynolds number, a trend resembling laminar predictions for flat plates or turbulent flow as opposed to laminar internal flow. It can also be observed that the Nusselt numbers are lower than conventional predictions for laminar flow, for example, a square channel will be expected to have Nu =3.66 under a constant temperature boundary condition and Nu = 4.36 under a constant heat flux boundary condition. It should be noted that the entry length for all tests in the present study was less than 20% of channel length; its effects can therefore be neglected [9].

Nusselt numbers of this order have been observed by several scholars who have experimentally and/or numerically studied heat transfer in miniaturised channels, for example, Dixit and Ghosh [21], Qu et al [10], Peng et al.[22] and Wu and Cheng [23] . Also, Reynolds number dependent Nusselt number correlations for miniaturised channels have been proposed by Choi et al. [24], Peng and Peterson [25] and Peng et al.[22]. Most of the explanations for these heat transfer behaviour in miniaturised channels can be classified as scaling effects [9, 18]. Most of the scaling effects often cited for low Nusselt

numbers are directly affected by the flow velocity. For example, Maranzana et al.[14] and Oyinlola et al. [13] showed that the effect of conjugate heat transfer diminishes as the Reynolds number increases. Another factor that may be responsible for the lower Nusselt numbers is wettability; due to low flow velocities, fluid contact with channel walls may be slightly minimised thus reducing the rate of heat transfer.

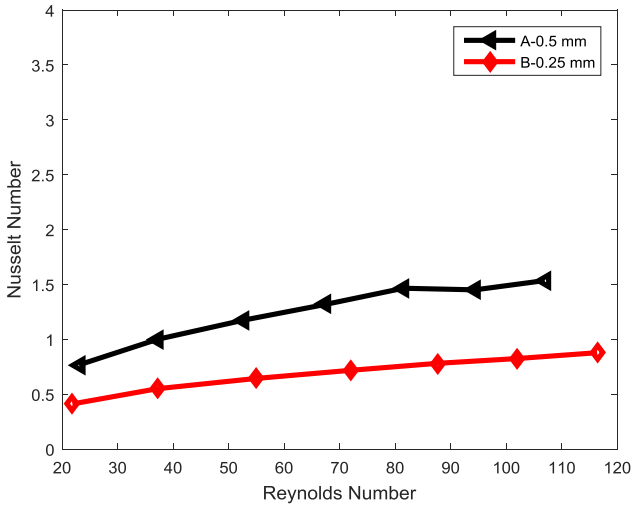

Figure 4 Nusselt number versus Reynolds number at 40°C

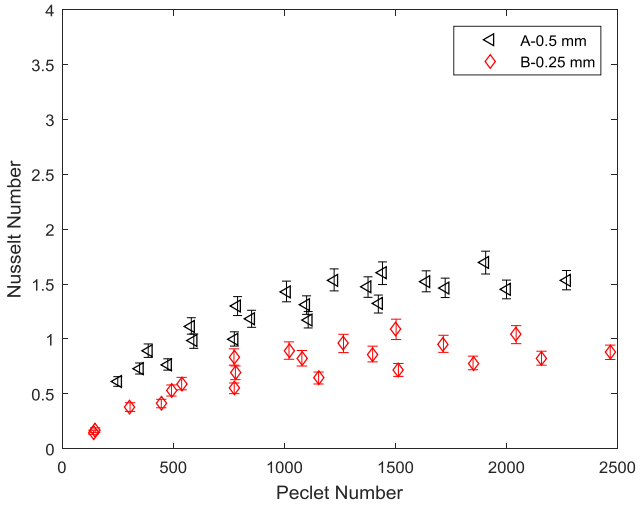

Figure 5 Nusselt number versus Peclet number

Figure 5 shows a plot of the Nusselt number versus Peclet numbers. These data points were obtained at various temperatures (5-40°C) and flow rates ($0<Re<100$). A plot of Nusselt number against Peclet number ($RePr$) is of importance because, depending on the thermal fluid used, fluid properties can vary significantly with temperature. It can be observed from Figure 5 that the Nusselt number is a function of both the Peclet Number and the geometry. A correlation was obtained using the least squares method. The correlation is presented in equation (11) and a plot of the correlation against the data points is shown in Figure 6. This can be observed to be a close fit. The Nusselt number will therefore vary depending on the Peclet number and the Hydraulic diameter.

$$Nu_{cor} = 0.1 D_h Pe^{0.4} \tag{11}$$

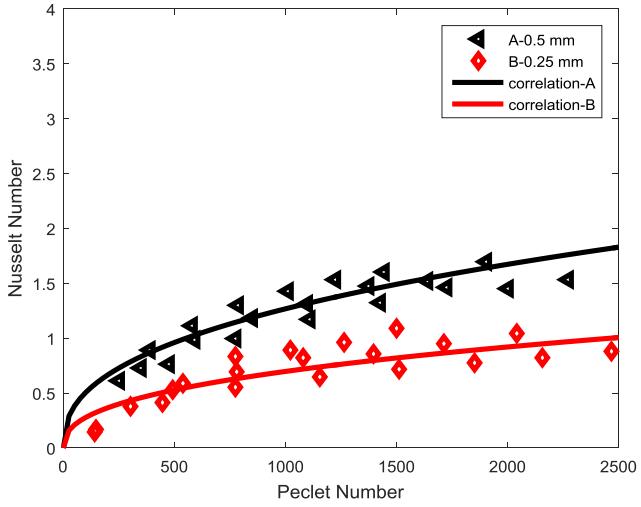

Figure 6 Nusselt number correlation

CONCLUSION

Forced convection experiments have been performed to investigate heat transfer in low Reynolds number flows through miniaturized channels. The measured Nusselt numbers were observed to be lower than conventional channels. Also, the Nusselt numbers were observed to depend more on the Peclet number and less on the geometry. Peclet number dependent Nusselt number was attributed to miniaturized scaling effects. A correlation for estimating the Nusselt number in terms of the Peclet number and hydraulic diameter was proposed. The results are significant in predicting the heat sinking performance in applications having low Reynolds number flows through miniaturized channels such as compact solar thermal collectors.

REFERENCES

[1] D. B. Tuckerman and R. F. W. Pease, "High-performance heat sinking for VLSI," vol. 2, pp. 126-129, 1981.

[2] K. Schubert, J. Brandner, M. Fichtner, G. Linder, U. Schygulla and A. Wenka, "Microstructure devices for applications in thermal and chemical process engineering," vol. 5, pp. 17-39, 2001.

[3] S. G. Kandlikar, *Heat Transfer and Fluid Flow in Minichannels and Microchannels.* Amsterdam, Netherlands; San Diego, CA; Oxford, UK: Elsevier, 2006.

[4] R. K. Shah and A. L. London, *Laminar Flow Forced Convection in Ducts : A Source Book for Compact Heat Exchanger Analytical Data.* New York: Academic Press, 1978.

[5] J. P. Holman, *Heat Transfer.* Boston, [Mass.]: McGraw Hill Higher Education, 2010.

[6] P. Wibulswas, "Laminar-flow heat-transfer in non-circular ducts," 1966.

[7] T. Dixit and I. Ghosh, "Review of micro- and mini-channel heat sinks and heat exchangers for single phase fluids," vol. 41, pp. 1298-1311, 2015.

[8] M. Asadi, G. Xie and B. Sunden, "A review of heat transfer and pressure drop characteristics of single and two-phase microchannels," vol. 79, pp. 34-53, 2014.

[9] P. Rosa, T. Karayiannis and M. Collins, "Single-phase heat transfer in microchannels: the importance of scaling effects," vol. 29, pp. 3447-3468, 2009.

[10] W. Qu, G. M. Mala and D. Li, "Heat transfer for water flow in trapezoidal silicon microchannels," vol. 43, pp. 3925-3936, 2000.

[11] P. Lee, S. V. Garimella and D. Liu, "Investigation of heat transfer in rectangular microchannels," vol. 48, pp. 1688-1704, 2005.

[12] M. Rahimi and R. Mehryar, "Numerical study of axial heat conduction effects on the local Nusselt number at the entrance and ending regions of a circular microchannel," vol. 59, pp. 87-94, 2012.

[13] M. A. Oyinlola, G. S. F. Shire and R. W. Moss, "Thermal analysis of a solar collector absorber plate with microchannels," *Exp. Therm. Fluid Sci.*, vol. 67, pp. 102-109, 10, 2015.

[14] G. Maranzana, I. Perry and D. Maillet, "Mini-and micro-channels: influence of axial conduction in the walls," vol. 47, pp. 3993-4004, 2004.

[15] V. V. Dharaiya and S. G. Kandlikar, "Numerical Investigation of Heat Transfer in Rectangular Microchannels Under H2 Boundary Condition During Developing and Fully Developed Laminar Flow," vol. 134, pp. 020911-020911, 2011.

[16] G. L. Morini, "Viscous dissipation as scaling effect for liquid flows in microchannels (keynote)," in *ASME 3rd International Conference on Microchannels and Minichannels*, 2005, pp. 93-102.

[17] G. L. Morini, "Single-phase convective heat transfer in microchannels: a review of experimental results," vol. 43, pp. 631-651, 2004.

[18] M. A. Oyinlola, G. S. F. Shire and R. W. Moss, "The significance of scaling effects in a solar absorber plate with micro-channels," *Appl. Therm. Eng.*, vol. 90, pp. 499-508, 11/5, 2015.

[19] J. P. Holman, *Experimental Methods for Engineers.* Boston: McGraw-Hill/Connect Learn Succeed, 2012.

[20] M. A. Oyinlola, G. S. F. Shire and R. W. Moss, "Investigating the effects of geometry in solar thermal absorber plates with micro-channels," *Int. J. Heat Mass Transfer*, vol. 90, pp. 552-560, 11, 2015.

[21] T. Dixit and I. Ghosh, "Low Reynolds number thermo-hydraulic characterization of offset and diamond minichannel metal heat sinks," vol. 51, pp. 227-238, 2013.

[22] X. Peng, G. Peterson and B. Wang, "Heat transfer characteristics of water flowing through microchannels," vol. 7, pp. 265-283, 1994.

[23] P. Wu and W. A. Little, "Measurement of the heat transfer characteristics of gas flow in fine channel heat exchangers used for microminiature refrigerators," vol. 24, pp. 415-420, 1984.

[24] S. B. Choi, R. R. Barren and R. Q. Warrington, "Fluid flow and heat transfer in micro-tubes," pp. 89-93, 1991.

[25] X. F. Peng and G. P. Peterson, "Convective heat transfer and flow friction for water flow in microchannel structures," vol. 39, pp. 2599-2608, 1996.